AGU ADVANCING EARTH AND SPACE SCIENCE

Geophysical Research Letters

RESEARCH LETTER
10.1029/2020GL089433

Key Points:
- Solar cell probe was used to investigate the lunar dust at CE-3 landing site for the first time
- The short-circuit current of lunar dust detector did not decrease sharply during the first several lunations
- In situ investigation results show no evidence for the existence of high concentrations of dust above the lunar terminators

Supporting Information:
- Supporting Information S1

Correspondence to:
X. Wang and Y. Wang,
rainer@163.com;
wyjlxlz@163.com

Citation:
Li, D., Wang, Y., Zhang, H., Wang, X., Wang, Y., Sun, Z., et al. (2020). In situ investigations of dust above the lunar terminator at the Chang'E-3 landing site in the Mare Imbrium. *Geophysical Research Letters*, *47*, e2020GL089433. https://doi.org/10.1029/2020GL089433

Received 25 MAR 2020
Accepted 16 AUG 2020
Accepted article online 28 AUG 2020

Detian Li and Yi Wang contributed equally to this work.

In Situ Investigations of Dust Above the Lunar Terminator at the Chang'E-3 Landing Site in the Mare Imbrium

Detian Li[1], Yi Wang[2], He Zhang[3], Xiaojun Wang[1], Yongjun Wang[1], Zezhou Sun[3], Jianhong Zhuang[2], Cunhui Li[2], Liping Chen[3], Haiyan Zhang[2], Xin Zou[3], Chao Zong[2], Hongyu Lin[4], Jinan Ma[3], Xiongyao Li[5], Xinyu Cui[6], Rijian Yao[2], Xilai Wang[2], Xin Gao[2], Shengsheng Yang[1], Xianrong Wang[2], and Biao Zhang[1]

[1]Science and Technology on Vacuum Technology and Physics Laboratory, Lanzhou Institute of Physics, China Academy of Space Technology, Lanzhou, China, [2]Science and Technology on Material Performance Evaluating in Space Environment Laboratory, Lanzhou Institute of Physics, China Academy of Space Technology, Lanzhou, China, [3]Beijing Institute of Spacecraft System Engineering, China Academy of Space Technology, Beijing, China, [4]Beijing Institute of Space Mechanics and Electricity, China Academy of Space Technology, Beijing, China, [5]State Key Laboratory of Environmental Geochemistry, Institute of Geochemistry, Chinese Academy of Sciences, Guiyang, China, [6]China Electric Technology Group Corporation, Tianjin Institute of Power Source, Tianjin, China

Abstract It was suspected that the horizon glow observed over the lunar terminator was caused by electrostatically levitated dust particles, but do high concentrations of dust particles really exist over the lunar terminator? This is an important question that cannot be answered even today. In fact, no in situ investigations about the lunar dust have been conducted on lunar surface since Apollo. Here we first report in situ investigations of lunar dust at Chang'E-3 (CE-3) landing site using solar cell probe (SCP). The results show that, different from Apollo's observation, the short-circuit current of SCP did not decrease sharply during the first several lunations except the first lunation, indicating the recently developed minimalist qualitative model of sunrise-driven dust transport might not be applicable at the geologically young CE-3 landing site. In addition, within detector's detection limit, no abrupt changes in dust concentration were observed above the sharp sunlight/shadow boundaries on lunar surface.

Plain Language Summary It was postulated for several decades that the lunar horizon glow observed during Apollo epoch was caused by forward scattering of sunlight by the electrostatically levitated dust particles above the sharp sunlight/shadow boundaries in the terminator zone. However, do high concentrations of charged dust particles really exist over the lunar terminator? This question cannot be definitively answered at present. China's Chang'E-3 (CE-3) mission provided a unique opportunity to address this long-standing scientific question because an in situ dust detector was loaded onto the lander. In this letter, the results obtained by the dust detector were demonstrated. It is found that the recently proposed minimalist model is not suitable for the geologically young CE-3 landing site. Within detector's detection limit, no putative high-density population of lunar dust particles was found above the sharp sunlight/shadow boundaries. This research, being carried out on the lunar surface rather than in orbit, can provide important new insights into the generation mechanisms about lunar horizon glow.

1. Introduction

The so-called lunar horizon glow observed five decades ago was the first space observation potentially generated by electrostatic dust lofting over the terminator region on the airless moon surface (Colwell et al., 2007; Rennilson & Criswell, 1974). However, the possible reasons for dust levitation and transport on airless moon are still actively debated in the lunar science community since there are no well-established physical mechanisms for producing such strong electric fields in the lunar environment to levitate charged dust particles over the sunrise and sunset terminators (O'Brien & Hollick, 2015; Szalay & Horányi, 2015; Wang et al., 2016). What is more, as of yet, it still remains unclear whether such charged lunar dust particles really exist above the lunar terminator (Horányi et al., 2015)? In order to provide more insights into the actual lunar dust environment, it is necessary to make reliable in situ dust explorations on the lunar surface. To date, however, the reports about in situ investigations of lunar dust on the moon surface are relatively few (Grün & Horányi, 2013; Li et al., 2019; O'Brien, 2009; O'Brien & Hollick, 2015; Yan et al., 2019) in

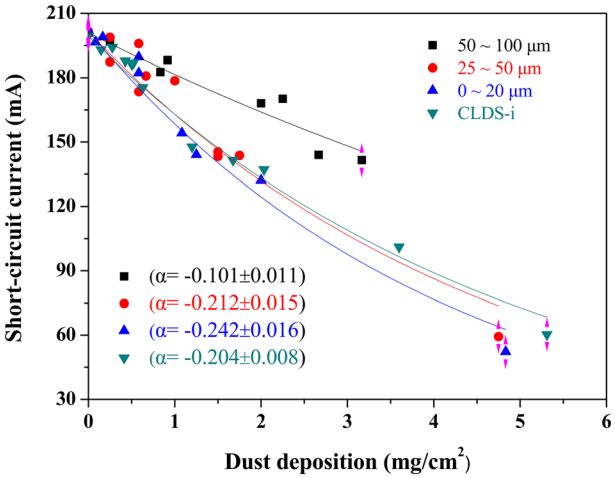

Figure 1. The dependence of short-circuit current of SCP on the deposition mass of lunar soil/dust simulants.

contrast with multiple searches carried out from lunar orbit over the past three decades (Barker et al., 2019; Feldman et al., 2014; Glenar et al., 2011, 2014; Grava et al., 2017; Horányi et al., 2015; Iglseder et al., 1996; Szalay & Horányi, 2015; Wooden et al., 2016; Zook & McCoy, 1991). Unlike the orbital investigations, in situ measurements made with lunar dust detector on the lunar surface can provide essential ground-truth data to validate or correct the results obtained from lunar orbiters as the latter significantly depend on the size and location of the putative lunar dust particles in most cases.

The China's Chang'E-3 (CE-3) mission was launched on 2 December 2013 and successfully landed at 44.12°N, 19.51°W in the Mare Imbrium on 14 December 2013 (UTC + 8), which was the first-ever soft landing on the lunar surface since the Soviet Union's Luna 24 mission in 1976 (Ling et al., 2015; Xiao et al., 2015). The lunar dust detector onboard CE-3 was China's first lunar dust detector actually used on the lunar surface, which primarily consisted of a sticky quartz crystal microbalance (SQCM) and a solar cell probe (SCP). The SQCM results were discussed detailedly in previous work (Li et al., 2019). Here, we only focus on the results obtained by SCP, which was dedicated to exploring the lunar dust principally caused by both anthropogenic and natural factors. The SCP, roughly 12 cm^2 in sensing area, was mainly constructed with a triple-junction GaInP/GaAS/Ge solar cell shielded by 0.12 mm silica, and its specific installation information is demonstrated in Figure S1 in the supporting information. The SCP was obviously distinct from the SQCM. On one hand, SQCM operated only during the day when the solar elevation angle was higher than ~20°, while the SCP could detect the lunar dust at any time during the entire CE-3 mission; thus, it can be used to learn about the lunar dust induced by the terminator crossings. Specifically, the SCP can be used to explore the putative high-density population of charged lunar dust lofted over the sharp sunlight/shadow boundaries during the total eclipse period. In this letter, the SCP was mainly used to investigate naturally occurring changes in dust accumulation over the mission lifetime, especially the role of lofted dust.

2. Instruments and Experiment

The operating principle of SCP was described by the so-called light occlusion model (Katzan & Edwards, 1991). The light occlusion model reflects the relationship between the short-circuit current of a dust-covered photovoltaic cell and the dust mass deposited on its surface and predicts an exponential decay in short-circuit current with dust accumulation. In present work, the relationships between deposition mass of lunar soil/dust simulants and the short-circuit current of SCP were investigated systematically. Here, the used lunar dust simulant, CLDS-i, contains ~75 vol.% of glass, ~15 vol.% of plagioclase, and 10 vol.% of olivine, pyroxene, ilmenite, and a little nanophase Fe^0, which is very close to that of Apollo low-Ti lunar mare dust (Tang et al., 2017). In addition, the simulated lunar dust particles have complicated shape and sharp edges. Thus, the CLDS-i has overall similarity to the Apollo lunar dust in chemistry, mineralogy, particle size, and morphology, and more detailed information about CLDS-i was described elsewhere (Tang et al., 2017). The used lunar soil simulant is CLRS-1 (i.e., CAS-1), which is chemically similar to Apollo 14 soil sample (Zheng et al., 2009). The CLRS-1 particles were sieved into three different size ranges of 50–100, 25–50, and 0–20 μm in order to evaluate the influence of particle size on the short-circuit current of SCP. The simulated sunlight was provided by a SpectroLab X-25 solar simulator with AM0 standard spectral irradiance (1,367 W/m^2), which was calibrated by a silicon reference standard prior to utilization. The response characteristics of the used solar cell covered with varying amounts of lunar soil/dust simulants were also investigated by using this SpectroLab X-25 simulator. The simulated sunlight was incident vertically on the cell surface; that is, the solar incidence angle (θ) relative to solar cell surface was normal. The lunar soil/dust simulants with different sizes were blown onto the clean solar cell surface using dry compressed air, and the short-circuit currents of solar cell under different deposition masses were monitored, and the results are given in Figure 1. The curve lines in Figure 1 were obtained by fitting of the corresponding experiment data for simulants with different size ranges, and the final expression is given as follows:

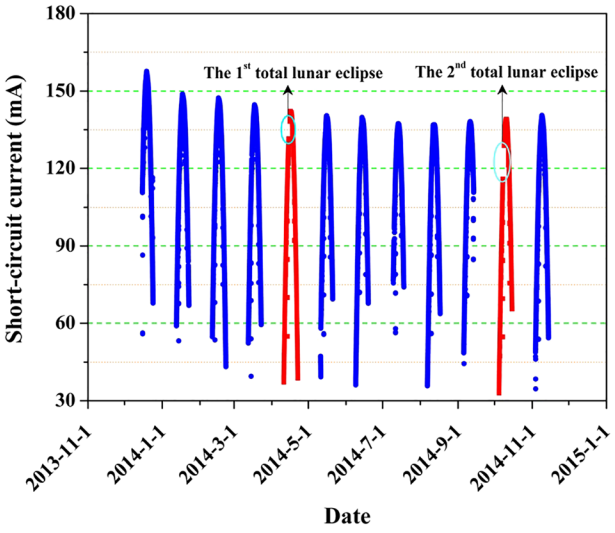

Figure 2. The variation of short-circuit current of SCP during the entire CE-3 mission. The data acquisition was stopped before the totality occurrence and restarted after the totality termination.

$$I = I_0 \cdot \exp(\alpha \cdot m_s). \tag{1}$$

Here, I_0 and I are the short-circuit currents (in mA) of solar cell before and after simulants deposition, respectively. I_0 is approximately equal to 200.58 ± 1.2 mA in our cases; m_s is the deposition mass of lunar soil/dust simulants in mg; α is a constant value related with size, shape, and distribution of the lunar soil/dust simulants; and the values of α for lunar soil simulant CLRS-1 with different size ranges of 50–100, 25–50, and 0–20 μm are −0.101, −0.212, and −0.242, respectively, and for lunar dust simulant CLDS-i is −0.204. According to Equation 1, m_s can be further expressed as follows:

$$m_s = \frac{\mathrm{Ln}(I_0) - \mathrm{Ln}(I)}{\alpha}. \tag{2}$$

It is important to note that Equation 2 is valid only for the present lunar soil/dust simulants. This is mainly due to the fact that the light occlusion efficiency of lunar soil/dust simulants is closely related with specific size, shape, and distribution of particles, and the small particles with large surface area-to-volume ratios have high occlusion efficiency (Katzan & Edwards, 1991; Katzan & Stidham, 1991; Said et al., 2018; Sayyah et al., 2014). In the actual tests on the lunar surface, the specific size, shape, and distribution of lunar dust particles deposited on cell surface are unknown, and consequently, the dust mass deposited on solar cell surface calculated from Equation 2 would have significant uncertainty.

The mass sensitivity, S, of the solar cell detector is defined as

$$S = -\frac{dI}{dm_s} = -\alpha \cdot I. \tag{3}$$

Thus, the mass sensitivity, S_0, of SCP for simulant CLDS-i ($\alpha = -0.204$) at an initial short-circuit current, I_0, of 199.37 mA is 40.67 mA/mg, and the minimum detectable mass of flight solar cell sensor can be further calculated as follows:

$$m_{\min} = \frac{I_{\min}}{S}. \tag{4}$$

Here, $I_{\min}$ is the minimum detectable current in SCP circuit, and the short-circuit current that can be accurately measured in SCP circuit is 0.1 mA. Thus, the minimum detectable mass of SCP is ~0.205 μg/cm^2, corresponding to ~2.46 μg for the full sensing area.

3. Results and Discussion

The SCP was installed on the top of the CE-3 lander, facing upward direction, to explore simultaneously lunar dust particles from different directions during the entire CE-3 mission. In reality, the real-time data acquisition was conducted only in lunar daytime as the solar elevation angle (θ) reached a certain value (~20°). In addition, the data acquisition of SCP must share time allocations with the other main payloads onboard CE-3 lander due to their scientific priority, and finally, about 160,000 short-circuit current values were recorded during the entire CE-3 mission, at a cadence of about 1 min. The detailed time periods for data acquisition are listed in Table S1.

Figure 2 demonstrates the annual variation of short-circuit current of SCP during the entire CE-3 mission. Here, the missing data points in the fifth and eleventh lunar daytimes, marked by cyan ellipse, are due to the occurrences of two total lunar eclipses. In order to correct for trends in solar irradiance, mainly originating from the different Sun-Earth distances, during the entire CE-3 mission, the solar irradiances in the following 11 lunar daytimes were normalized using the value in the first lunar daytime as a

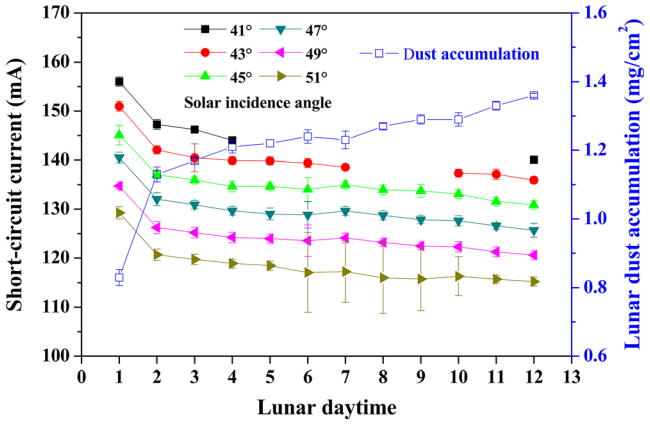

Figure 3. The variation of short-circuit current, collected in 1° bin widths, of SCP with different solar incidence angles and the averaged deposition mass of lunar dust in each lunar daytime during the CE-3 mission.

reference (see Figure S5). Thus, all the short-circuit current values recorded from the second to twelfth lunar daytimes in Figure 2 were converted at the identical solar irradiance as that of the first lunar daytime in order to facilitate comparison. It is clearly seen that the maximum short-circuit current, reached at local noon of each lunar daytime, decreased gradually from the first to ninth lunar daytimes and then increased subsequently during the remaining test period. This trend was mainly caused by both the different minimum solar incidence angles that can reach at the CE-3 landing site in each lunar daytime during the whole CE-3 mission period (see Figure S6) and the lunar dust deposition together. In order to isolate the influence of lunar dust accumulation, measured short-circuit currents are collected in narrow bins around specific values of solar incidence angle as illustrated in Figure 3. The averaged deposition mass of lunar dust is superimposed.

In reality, during the entire CE-3 mission, the minimum solar incidence angle, capable of reaching the CE-3 landing site, increased from ~41.09° to ~44.14° as the Earth-Moon system moved from its January perihelion to its July aphelion, and then to 41.34° when the system approached its perihelion again in the coming year. Therefore, for solar incidence angle of 41°, the missing data points from the fifth to eleventh lunar daytimes are ascribed to the fact that the solar incidence angles cannot reach the values <42° in CE-3 landing site during those lunar daytimes. This is also the very reason for the missing data points from the eighth to ninth lunar daytimes for solar incidence angle of 43°.

Figure 3 indicates a significant reduction in short-circuit current between the first two lunar daytimes, and then the short-circuit current gradually reduced over the remaining 11 lunar daytimes. In this situation, the primary reason for the initial reduction of short-circuit currents during the first two lunar daytimes was ascribed to the anthropogenic causes—CE-3 landing and Rover's activities, the former disrupted a relatively large region and stirred up considerable lunar dust (Li et al., 2014). Deposition of the resulting lunar dust, debris, rocket exhaust products, and dust thrown up by the Yutu's wheels as well as dust that fell from directional antenna together resulted in a significant reduction of short-circuit current between the first two lunar daytimes. In subsequent lunations, the naturally occurring dust deposition was mainly responsible for the slight decrease of short-circuit current from the second to twelfth lunar daytimes. Of course, the long-term space radiation can also damage solar cell performance and reduce short-circuit current even though the used solar cell shielded by silica glass is an insensitive radiation instruments. The total degradation caused by space radiation during whole CE-3 1-year mission period was only 1.6% of the initial value (see Figure S8). The averaged deposition mass of lunar dust in each lunation during the entire CE-3 mission was also roughly estimated by using Equation 2, and in this process, the α (~0.204) for lunar dust simulant CLDS-i was used. It is clearly seen from Figure 3 that the averaged deposition masses in the first two lunations were ~0.83 and ~0.30 mg/cm^2, respectively. However, the total deposition mass from the second to twelfth lunations, that is, naturally occurring dust deposition, was only ~0.23 mg/cm^2. This value can be further corrected by considering the short-circuit current reduction caused by space radiation damage of solar cell, and a value of ~0.15 mg/cm^2 would be more appropriate for natural dust deposition from the second to twelfth lunations.

The lunar horizon glow observed from orbit by Apollo astronauts at both sunrise and sunset terminators has been attributed to sunlight scattering by electrostatically levitated and transported dust above the lunar terminators. However, this scenario is still being debated (Berg et al., 1976; Colwell et al., 2007; O'Brien, 2011; Popel et al., 2018; Rennilson & Criswell, 1974; Stubbs et al., 2006; Zook & McCoy, 1991). To date, however, no hard evidence for the putative high-density population of lunar dust particles above the terminator has been obtained to support the Apollo epoch observations. In recent years, in situ dust detector measurements do not support the previous viewpoints (Horányi et al., 2015; Szalay & Horányi, 2015) and some new understandings about early experiment results that thought to be linked with lunar dust at that time (Glenar et al., 2014; Grün & Horányi, 2013). In more recent years, it is now generally accepted that the cohesive cohesion, acting among micron-size lunar dust particles, plays an important role in determining how the lunar dust particles get into the lunar exosphere and the electrostatic repulsion forces among the like-charged

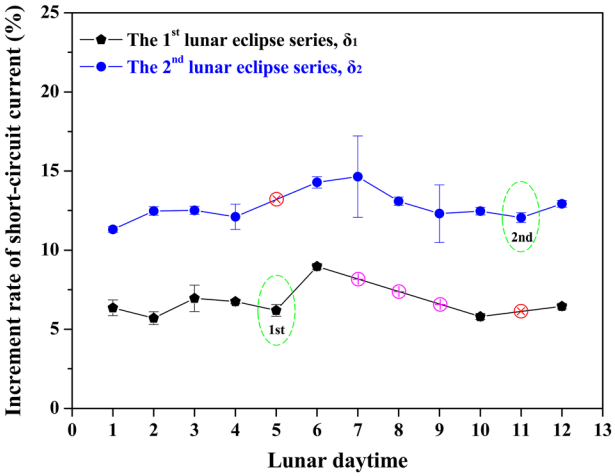

Figure 4. Increment rate of short-circuit current δ_1 and δ_2 computed at each lunar day. Values show the fractional difference in SCP current between posteclipse and pre-eclipse solar incidence angles (see the text for definitions). Significant changes in accumulated dust due to an eclipse would appear as an abrupt discontinuity on eclipse day. However, neither of the eclipse events show a noticeable deviation. Here, the data acquisitions for the first and second total lunar eclipses stopped at solar incidence angles of 46.60° and 51.65° and restarted at 43.37° and 45.33°, respectively. ⊗ represents the lunar daytimes in which the short-circuit currents cannot be recorded due to the occurrence of totality, and ⊕ represents the lunar daytimes in which the minimum solar incidence angles in CE-3 landing site did not reach 43.37°.

objects are too weak to overcome the cohesive and gravitational forces acting on them totally (Szalay & Horányi, 2015; Yan et al., 2019). Consequently, the electrostatic lofting mechanism seems to be less efficient than previously thought. This is the most probable reason why the putative high-density population of lunar dust particles above the lunar terminators was not detected in several recent missions (Barker et al., 2019; Feldman et al., 2014; Glenar et al., 2014; Horányi et al., 2015). In 2015, on the basis of the existing models, O'Brien et al. developed a minimalist qualitative model to describe the dust particle movement in the complex lunar surface plasma environment (O'Brien & Hollick, 2015). In that model, the fine lunar dust particles, being freed from strong particle-to-particle cohesive forces via rocket exhaust jet interaction with lunar surface, could be lofted to a certain height due to the electrostatic repulsion of like-charged lunar surface and dust particles during the next several sunrises (O'Brien & Hollick, 2015). This model can well explain the rapid reduction of short-circuit current of solar cells (Bates & Fang, 2001; Hollick & O'Brien, 2013) as well as sunrise-driven dust storms (O'Brien & Hollick, 2015) during the first several lunations. However, this model cannot accurately account for experimental phenomenon observed in present work. On one hand, just like the Apollo 12 landing site, CE-3 landing site was also significantly disrupted by CE-3 rocket exhaust during descent stage, and consequently, substantial amounts of lunar dust particles were liberated from lunar surface (Li et al., 2014; Zhang et al., 2015). However, as shown in Figure 3, unlike the Apollo's quicker degradation of short-circuit current over the first five lunations stage, the SCP's current showed significant degradation between the first and the second lunations due to the deposition of dust particles kicked-up during CE-3 descent stage, after that, and the SCP's current showed an almost linear decrease during the last 11 lunar daytimes, indicating that the electrostatically lofted lunar dust particles described by the minimalist qualitative model did not actually exist at least in the geologically young CE-3 landing site (Fa et al., 2015; Ling et al., 2015; Xiao et al., 2015; Yan et al., 2019).

The total lunar eclipses provided precious opportunity to confirm whether or not the lunar dust could be electrostatically lofted and transported due to the passage of sharp sunlight/shadow boundaries. This is because the occurrence of a total lunar eclipse provided a highly imitated occasion where the sunrise and sunset successively occurred in a relatively short timescale. Fortunately, two total lunar eclipses occurred during the CE-3 mission, and thus, the sharp sunlight/shadow boundaries, just like terminator, moved across the place where CE-3 landed twice for each total lunar eclipse. To describe the influence of the eclipses on dust accumulation, we define short-circuit current increment rates, δ_1 (for the first lunar totality, occurred in the fifth lunar day) and δ_2 (for the second lunar totality, occurred in the eleventh lunar day), which is the fractional change in short-circuit current during each eclipse event. Here, the increment rate for the first total lunar eclipse is calculated as follows: $\delta_1 = \frac{I_{(43.47°)} - I_{(46.60°)}}{I_{(46.60°)}}$, where, $I_{(43.37°)}$ and $I_{(46.60)}$ are the short-circuit currents averaging all the recorded current values collected in 0.5° bin widths of solar incidence angles before and after the first totality (i.e., $I_{(43.47°)}$ is the short-circuit current averaging all the recorded current values in the incidence angle range from 43.37° to 42.97°; $I_{(46.60°)}$ is the short-circuit current averaging all the recorded current values in the range from 47.10° to 46.60°). For the second total lunar eclipse, $\delta_2 = \frac{I_{(45.33°)} - I_{(51.65°)}}{I_{(51.65°)}}$, which is calculated in the same way as for δ_1. For comparison, the increment rates in the other lunar daytimes without a lunar eclipse are also given. However, the significant dust deposition did not happen for any total lunar eclipse, as discussed below.

Figure 4 gives the increment rates of short-circuit currents of SCP defined at the two totalities, as described above. It can be expected that if the putative high-density population of lunar dust particles over the sharp sunlight/shadow boundaries really exists, the increment rate of SCP's short-circuit current would decrease inevitably once the sharp sunlight/shadow boundaries move across the CE-3 landing site due to the

deposition of large amounts of lofted dust particles. However, it is clear that the increment rates of short-circuit currents before and after two totalities did not change significantly in contrast to other cases, implying that the lunar dust levitation and transport due to the passages of the sharp sunlight/shadow boundaries on the moon surface were not as influential as anticipated from Apollo epoch. This conclusion drawn from in situ dust investigation on lunar surface is also consistent with the recent reanalysis of the LEAM experiment (Grün & Horányi, 2013) as well as the results obtained by Clementine (Glenar et al., 2014), Lunar Dust Experiment (LDEX) (Horányi et al., 2015; Szalay & Horányi, 2015) and Lyman-Alpha Mapping Project (LAMP) (Feldman et al., 2014) from lunar orbits. The exact physical reasons for the absence of high concentrations of lunar dust particles over the sharp sunlight/shadow boundaries in CE-3 landing site are not yet fully understood; however, the weak dust activity in the geologically young CE-3 landing region (Yan et al., 2019) and the lack of strong electric field forces on the lunar surface for lunar dust particles to overcome gravity and cohesion (Popel et al., 2018; Szalay & Horányi, 2015; Wang et al., 2016) are the two most likely causes. However, it cannot be entirely ruled out that high concentrations of lunar dust particles may still exist in the lower lunar space environment at altitudes below ~2.05 m because recent laboratory experiments showed that the inner walls of microcavities between dust particles can collect very large negative charge under electron beam or UV radiation conditions (Hood et al., 2018; Schwan et al., 2017; Wang et al., 2016), and the negatively charged dust particles can be electrostatically lofted by the repulsion from the adjacent like-charged particles to reach an equivalent height of ~0.11 m on the lunar surface, comparable to the height of the lunar horizon glow observed by Surveyors. Unfortunately, the SCP cannot detect dust particles at this height range. Given the minimum detectable mass limitation of the SCP, it can be concluded that the deposition of lunar dust induced by the sharp sunlight/shadow boundaries crossings at the CE-3 landing site with a height about 2.05 m is less than 2.46×10^{-3} mg for the full sensing area of SCP.

4. Conclusions

In conclusion, the lunar dust over the lunar terminator at the CE-3 landing site was investigated for the first time by using an in situ SCP. It is found that, except for initial dust fallback following the CE-3 landing, the short-circuit current of SCP did not decrease rapidly in the first several lunar daytimes in contrast to Apollo's exploration, indicating the electrostatically lofted lunar dust particles described by the minimalist qualitative model did not exist at least boundary crossings in the geologically young CE-3 landing site. In addition, the increment rate of short-circuit current during the sharp sunlight/shadow boundaries crossings did not significantly differ from other lunar daytimes without a lunar eclipse, which means that there was no putative high-density population of lunar dust particles over the sunlight/shadow boundaries. Lastly, the upper limit for dust deposition induced by the sharp sunlight/shadow boundaries crossings at the CE-3 landing site was less than 2.46×10^{-3} mg for the full sensing area of SCP. The relative weak dust activity and the lack of strong electric field force on the lunar surface for lunar dust particles to overcome gravity and cohesion are the two most probable reasons for the absence of high concentrations of lunar dust over the sunlight/shadow boundaries.

Data Availability Statement

All the data used in this manuscript can be obtained online (from https://doi.org/10.6084/m9.figshare.12845180).

Acknowledgments

Detian Li and Yongjun Wang acknowledge support of the Natural Science Foundation of China (Grant Nos. 61627805 and 61671226). Yongjun Wang thanks to the Equipment Pre-Research Foundation of Equipment Development Department of People's Republic of China Central Military Commission (Grant No. 6142207010704). The authors also thank two anonymous reviewers for their constructive comments and suggestions, which led to many improvements in the manuscript.

References

Barker, M. K., Mazarico, E., McClanahan, T. P., Sun, X., Neumann, G. A., Smith, D. E., et al. (2019). Searching for lunar horizon glow with the Lunar Orbiter Laser Altimeter. *Journal of Geophysical Research: Planets*, *124*, 2728–2744. https://doi.org/10.1029/2019JE006020

Bates, J. R., & Fang, P. H. (2001). Some astronomical effects observed by solar cells from Apollo missions on lunar surface. *Solar Energy Materials and Solar Cells*, *68*(1), 23–29. https://doi.org/10.1016/S0927-0248(00)00343-3

Berg, O. E., Wolf, H., & Rhee, J. (1976). *Lunar soil movement registered by the Apollo 17 Cosmic Dust Experiment* (pp. 233–237). Berlin, Heidelberg: Springer.

Colwell, J. E., Batiste, S., Horányi, M., Robertson, S., & Sture, S. (2007). Lunar surface: Dust dynamics and regolith mechanics. *Reviews of Geophysics*, *45*, RG2006. https://doi.org/10.1029/2005RG000184

Fa, W. Z., Zhu, M. H., Liu, T., & Plescia, J. B. (2015). Regolith stratigraphy at the Chang'E-3 landing site as seen by lunar penetrating radar. *Geophysical Research Letters*, *42*, 179–187. https://doi.org/10.1002/2015GL066537

Feldman, P. D., Glenar, D. A., Stubbs, T. J., Retherford, K. D., Randall Gladstone, G., Miles, P. F., et al. (2014). Upper limits for a lunar dust exosphere from far-ultraviolet spectroscopy by LRO/LAMP. *Icarus*, *233*, 106–113. https://doi.org/10.1016/j.icarus.2014.01.039

Glenar, D. A., Stubbs, T. J., Hahn, J. M., & Wang, Y. (2014). Search for a high-altitude lunar dust exosphere using Clementine navigational star tracker measurements. *Journal of Geophysical Research: Planets*, *119*, 2548–2567. https://doi.org/10.1002/2014JE004702

Glenar, D. A., Stubbs, T. J., McCoy, J. E., & Vondrak, R. R. (2011). A reanalysis of the Apollo light scattering observations, and implications for lunar exospheric dust. *Planetary and Space Science*, *59*(14), 1695–1707. https://doi.org/10.1016/j.pss.2010.12.003

Grava, C., Stubbs, T. J., Glenar, D. A., Retherford, K. D., & Kaufmann, D. E. (2017). Absence of a detectable lunar nanodust exosphere during a search with LRO's LAMP UV imaging spectrograph. *Geophysical Research Letters*, *44*, 4591–4598. https://doi.org/10.1002/2017GL072797

Grün, E., & Horányi, M. (2013). A new look at Apollo 17 LEAM data: Nighttime dust activity in 1976. *Planetary and Space Science*, *89*, 2–14. https://doi.org/10.1016/j.pss.2013.10.005

Hollick, M., & O'Brien, B. J. (2013). Lunar weather measurements at three Apollo sites 1969–1976. *Space Weather*, *11*, 651–660. https://doi.org/10.1002/2013SW000978

Hood, N., Carroll, A., Mike, R., Wang, X., Schwan, J., Hsu, H. W., & Horányi, M. (2018). Laboratory investigation of rate of electrostatic dust lofting over time on airless planetary bodies. *Geophysical Research Letters*, *45*, 13,206–13,212. https://doi.org/10.1029/2018GL080527

Horányi, M., Szalay, J. R., Kempf, S., Schmidt, J., Grün, E., Srama, R., & Sternovsky, Z. (2015). A permanent, asymmetric dust cloud around the Moon. *Nature*, *522*(7556), 324–326. https://doi.org/10.1038/nature14479

Iglseder, H., Uesugi, K., & Svedhem, H. (1996). Cosmic dust measurements in lunar orbit. *Advances in Space Research*, *17*(12), 177–182. https://doi.org/10.1016/0273-1177(95)00777-C

Katzan, C. M., & Edwards, J. L. (1991). Lunar dust transport and potential interactions with power system components, NASA Contractor Rep., 4404, United States.

Katzan, C. M., & Stidham, C. R. (1991). Lunar dust interactions with photovoltaic arrays, paper presented at The Conference Record of the Twenty-Second IEEE Photovoltaic Specialists Conference - 1991, 7–11 Oct. 1991, https://doi.org/10.1109/PVSC.1991.169464

Li, C. L., Mu, L. L., Zou, X. D., Liu, J. J., Ren, X., Zeng, X. G., et al. (2014). Analysis of the geomorphology surrounding the Chang'E-3 landing site. *Research in Astronomy and Astrophysics*, *14*(12), 1514–1529. https://doi.org/10.1088/1674-4527/14/12/002

Li, D., Wang, Y., Zhang, H., Zhuang, J., Wang, X., Wang, Y., et al. (2019). In-situ measurements of lunar dust at the Chang'E-3 landing site in the northern Mare Imbrium. *Journal of Geophysical Research: Planets*, *124*, 2168–2177. https://doi.org/10.1029/2019JE006054

Ling, Z., Jolliff, B. L., Wang, A., Li, C., Liu, J., Zhang, J., et al. (2015). Correlated compositional and mineralogical investigations at the Chang'E-3 landing site. *Nature Communications*, *6*, 8880. https://doi.org/10.1038/ncomms9880

O'Brien, B. J. (2009). Direct active measurements of movements of lunar dust: Rocket exhausts and natural effects contaminating and cleansing Apollo hardware on the Moon in 1969. *Geophysical Research Letters*, *36*, L09201. https://doi.org/10.1029/2008GL037116

O'Brien, B. J. (2011). Review of measurements of dust movements on the Moon during Apollo. *Planetary and Space Science*, *59*(14), 1708–1726. https://doi.org/10.1016/j.pss.2011.04.016

O'Brien, B. J., & Hollick, M. (2015). Sunrise-driven movements of dust on the Moon: Apollo 12 ground-truth measurements. *Planetary and Space Science*, *119*, 194–199. https://doi.org/10.1016/j.pss.2015.09.018

Popel, S. I., Zelenyi, L. M., Golub, A. P., & Dubinskii, A. Y. (2018). Lunar dust and dusty plasmas: Recent developments, advances, and unsolved problems. *Planetary and Space Science*, *156*, 71–84. https://doi.org/10.1016/j.pss.2018.02.010

Rennilson, J. J., & Criswell, D. R. (1974). Surveyor observations of lunar horizon-glow. *The Moon*, *10*(2), 121–142. https://doi.org/10.1007/BF00655715

Said, S. A. M., Hassan, G., Walwil, H. M., & Al-Aqeeli, N. (2018). The effect of environmental factors and dust accumulation on photovoltaic modules and dust-accumulation mitigation strategies. *Renewable and Sustainable Energy Reviews*, *82*, 743–760. https://doi.org/10.1016/j.rser.2017.09.042

Sayyah, A., Horenstein, M. N., & Mazumder, M. K. (2014). Energy yield loss caused by dust deposition on photovoltaic panels. *Solar Energy*, *107*, 576–604. https://doi.org/10.1016/j.solener.2014.05.030

Schwan, J., Wang, X., Hsu, H. W., Grün, E., & Horányi, M. (2017). The charge state of electrostatically transported dust on regolith surfaces. *Geophysical Research Letters*, *44*, 3059–3065. https://doi.org/10.1002/2017GL072909

Stubbs, T. J., Vondrak, R. R., & Farrell, W. M. (2006). A dynamic fountain model for lunar dust. *Advances in Space Research*, *37*(1), 59–66. https://doi.org/10.1016/j.asr.2005.04.048

Szalay, J. R., & Horányi, M. (2015). The search for electrostatically lofted grains above the Moon with the Lunar Dust Experiment. *Geophysical Research Letters*, *42*, 5141–5146. https://doi.org/10.1002/2015GL064324

Tang, H., Li, X., Zhang, S., Wang, S., Liu, J., Li, S., et al. (2017). A lunar dust simulant: CLDS-i. *Advances in Space Research*, *59*(4), 1156–1160. https://doi.org/10.1016/j.asr.2016.11.023

Wang, X., Schwan, J., Hsu, H. W., Grün, E., & Horányi, M. (2016). Dust charging and transport on airless planetary bodies. *Geophysical Research Letters*, *43*, 6103–6110. https://doi.org/10.1002/2016GL069491

Wooden, D. H., Cook, A. M., Colaprete, A., Glenar, D. A., Stubbs, T. J., & Shirley, M. (2016). Evidence for a dynamic nanodust cloud enveloping the Moon. *Nature Geoscience*, *9*(9), 665–668. https://doi.org/10.1038/ngeo2779

Xiao, L., Zhu, P., Fang, G., Xiao, Z., Zou, Y., Zhao, J., et al. (2015). A young multilayered terrane of the northern Mare Imbrium revealed by Chang'E-3 mission. *Science*, *347*(6227), 1226–1229. https://doi.org/10.1126/science.1259866

Yan, Q., Zhang, X., Xie, L., Guo, D., Li, Y., Xu, Y., et al. (2019). Weak dust activity near a geologically young surface revealed by Chang'E-3 Mission. *Geophysical Research Letters*, *46*, 9405–9413. https://doi.org/10.1029/2019GL083611

Zhang, J. H., Yang, W., Hu, S., Lin, Y., Fang, G., Li, C., et al. (2015). Volcanic history of the Imbrium basin: A close-up view from the lunar rover Yutu. *Proceedings of the National Academy of Sciences of the United States of America*, *112*(17), 5342–5347. https://doi.org/10.1073/pnas.1503082112

Zheng, Y. C., Wang, S., Ouyang, Z., Zou, Y., Liu, J., Li, C., et al. (2009). CAS-1 lunar soil simulant. *Advances in Space Research*, *43*(3), 448–454. https://doi.org/10.1016/j.asr.2008.07.006

Zook, H. A., & McCoy, J. E. (1991). Large scale lunar horizon glow and a high altitude lunar dust exosphere. *Geophysical Research Letters*, *18*(11), 2117–2120. https://doi.org/10.1029/91GL02235

References From the Supporting Information

Bretagnon, P., & Francou, G. (1988). Planetary theories in rectangular and spherical variables—VSOP 87 solutions. *Astronomy and Astrophysics*, *202*(1–2), 309–315.

Chapront-Touze, M., & Chapront, J. (1983). The lunar ephemeris ELP 2000. *Astronomy and Astrophysics*, *124*(1), 50–62.

Davies, M. E., & Colvin, T. R. (2000). Lunar coordinates in the regions of the Apollo landers. *Journal of Geophysical Research*, *105*(E8), 20,277–20,280. https://doi.org/10.1029/1999JE001165

Li, X., Wang, S., Zheng, Y., & Cheng, A. (2008a). A lunar surface effective solar irradiance real-time model. *Chinese Journal of Geophysics*, *51*(1), 25–33. https://doi.org/10.1002/cjg2.1191

Li, X., Wang, S., Zheng, Y., & Cheng, A. (2008b). Estimation of solar illumination on the Moon: A theoretical model. *Planetary and Space Science*, *56*(7), 947–950. https://doi.org/10.1016/j.pss.2008.02.008

Maxwell, E. L. (1998). METSTAT—The solar radiation model used in the production of the National Solar Radiation Data Base (NSRDB). *Solar Energy*, *62*(4), 263–279. https://doi.org/10.1016/S0038-092X(98)00003-6

Meeus, J. (1991). *Astronomical Algorithms*. Virginia: Willmann-Bell Inc.

Owczarek, S. (1997). Vector model for calculation of solar radiation intensity and sums incident on tilted surfaces. Identification for the three sky condition in Warsaw. *Renewable Energy*, *11*(1), 77–96. https://doi.org/10.1016/S0960-1481(96)00117-6